Case Studies in Construction Materials 25 (2026) e06280

Contents lists available at ScienceDirect

Case Studies in Construction Materials

journal homepage: www.elsevier.com/locate/cscm

Case study

Quantifying construction-stage (A5) energy consumption in mass timber buildings: A dual-track assessment framework

Baowen Zhang [a,c], Hongmei Gu [b], Paul Crovella [a,d,*]

[a] Department of Sustainable Resources Management, SUNY College of Environmental Science and Forestry, 1 Forestry Dr., Syracuse, 13210, NY, USA
[b] U.S. Department of Agriculture, Forest Service, Forest Products Laboratory, One Gifford Pinchot Drive, Madison, 53726, WI, USA
[c] School of Engineering, Colorado State University Pueblo, 2200 Bonforte Blvd, Pueblo, 81001, CO, USA
[d] Syracuse Center of Excellence, 727 E Washington St, Syracuse, 13244, NY, USA

ARTICLE INFO

Keywords:
Mass timber construction
Construction-stage energy
Life-cycle assessment
Monte Carlo simulation
Learning curve
Cross-system comparison
Cold-climate construction

ABSTRACT

The building sector accounts for approximately 37% of global energy-related carbon emissions, and as operational efficiency improves, the share attributable to embodied carbon continues to grow. Mass timber has emerged as a promising structural alternative because of its lower embodied carbon, biogenic carbon storage, and potential to accelerate construction schedules. However, construction-stage energy use (A5) is often oversimplified in building life-cycle assessment, with previous studies frequently approximating it as a fixed percentage (~3%) of total embodied energy rather than explicitly inventorying on-site activities. To address this gap, this study develops a dual-track framework for quantifying A5 energy use, combining a theoretical lower bound with a schedule-based upper bound and Monte Carlo uncertainty analysis. Crucially, this study evaluates A5 as a standalone module and does not assess its relative contribution within the full life-cycle profile of the buildings. The framework is applied to two completed large-scale mass timber projects in the U.S. Midwest (ASHRAE Climate Zone 5A) and extended to functionally equivalent reinforced concrete (RC) and structural steel options. Results show that in cold-climate projects, temporary heating dominates A5 energy use (52%–60%), while mechanical fastener installation contributes less than 0.2% regardless of climate. Compared with functionally equivalent alternatives in the same climate zone, mass timber achieves approximately 30% lower A5 energy use than RC and approximately 13% lower than structural steel. A complementary climate-sensitivity analysis extends the framework across ASHRAE Climate Zones 1A through 5A and shows that the mass timber advantage holds across this range, although the absolute A5 totals decline substantially as temporary-heating demand diminishes. In addition, a 44% learning-curve productivity improvement in cross-laminated timber (CLT) installation suggests further potential for reducing construction-stage energy consumption. External validation using Bakers Place, another completed mass timber project, supports the transferability of the methodology, with observed values for all three structural systems falling within their respective 90% credible intervals. These findings indicate that A5 energy use in cold-climate mass timber projects has been substantially under-quantified in previous studies and that the proposed framework provides a systematic method for evaluating construction-stage energy impacts.

* Corresponding author at: Department of Sustainable Resources Management, SUNY College of Environmental Science and Forestry, 1 Forestry Dr., Syracuse, 13210, NY, USA.

E-mail address: plcrovella@esf.edu (P. Crovella).

https://doi.org/10.1016/j.cscm.2026.e06280
Received 3 April 2026; Received in revised form 25 May 2026; Accepted 26 June 2026

Available online 1 July 2026

1. Introduction

Buildings account for a substantial share of global energy-related greenhouse-gas (GHG) emissions, placing the sector at the center of national and corporate decarbonization agendas arising from the Paris Agreement [1]. Accounting for roughly 40% of energy-related GHG emissions, buildings have made the construction industry a focal point for sustainable practices [2–6]. To evaluate decarbonization scales of buildings, the construction sector relies on the standardized, science-based life-cycle assessment (LCA). When applying LCA to buildings in North America, practice primarily follows ISO 14040:2006 and ISO 14044:2006, which organize life-cycle information into product (A1–A3), construction (A4–A5), use (B1–B7), end-of-life (C1–C4), and beyond-the-system (D) stages, with module D capturing reuse, recovery, and recycling potentials. Research has shown that about 11% of society's GHG emissions arise from manufacturing building materials such as steel, cement, and glass [7]. Over the past decade, numerous studies have investigated the environmental impacts of alternative structural materials [8–12]. Among these, mass timber has attracted attention from building developers due to its lower weight and embodied carbon [13], its renewability in North America [14], and its biogenic carbon storage benefits [15]. In construction practice, a high degree of off-site prefabrication and material handling have been reported to accelerate onsite erection—on the order of ~20% in some cases, while reducing noise and waste relative to concrete and steel building projects [16]. Distinct from light-frame timber used in single-family detached housing, mass timber is applied in commercial, multi-family, and institutional buildings. Its North American adoption is driven by both major technology companies such as Apple, Amazon, and Alphabet and a growing number of smaller privately funded mid-rise developers [17]. Despite growing adoption, especially in larger, taller projects, quantifying the GHG implications of substituting mass timber for concrete or steel remains methodologically heterogeneous, and consensus on standardized quantification, particularly for the A5 construction stage, is still developing [18]. Currently, studies on the LCA of timber construction have not reached a harmonized procedure across regions because of differences in climatic characteristics, standards (e.g., ISO 14040/14044; EN 15804/15978/16485), population structures, and building cultures. In Europe, especially Northern Europe (such as Sweden and Norway)—EN standards are widely adopted. Due to proximity to mature manufacturing of mass timber products and a long tradition of using timber as a building material, this region has produced the most studies of using LCA to quantify mass timber buildings (accounting for roughly half of the studies reviewed by the authors).

Although numerous studies have assessed the embodied carbon of mass timber buildings across these regions, few have explicitly quantified the A5 construction stage as a standalone module. Takano et al. reviewed EN standard documents and attempted to develop a standardized process to guide future carbon-emission assessments. They quantified the carbon emissions of a building with LVL and glulam columns and beams to verify the feasibility of this process, pointing out that LCA, as a data-intensive method, requires substantial practical data and feedback to prove its generalizability [19]. Dodoo et al. analyzed the life-cycle carbon implications of three timber-frame multi-storey buildings, verifying that low-energy designs (LVL with a CLT elevator shaft) can save approximately 9% of carbon emissions over a 50-year lifespan [20]. Moncaster et al. focused on the sensitivity of LCA applied to building materials and structures. They compared buildings of the same scale made with concrete frame, steel frame, load-bearing masonry, and CLT, and examined which part of the structure, shell, and interior finishes had the most significant embodied-carbon contribution. They concluded that CLT performed the best in carbon reduction (often less than half of the emissions of the remaining structures) and noted uncertainty around which sub-assemblies dominate depending on the structural design [21]. A notable feature of these European studies is that the substructure (foundations) is rarely included, and because of settlement patterns, many studies focus on single-family houses, with very few covering buildings over 1000 m^2; consequently, A5 is rarely reported as a standalone module in this region. Early comparative evidence on construction-stage energy use also indicates system-dependent differences: steel sites tend to be lowest, concrete highest (occasionally by orders of magnitude), and timber in between (often ~2–3× steel), which further suggests that A5 should be explicitly inventoried rather than represented by a fixed percentage.

In the Americas, with North America accounting for the vast majority of studies, the building cases studied are concentrated in "timber-hub" cities (Portland, Seattle, Montréal). Pierobon et al. selected the Pacific Northwest as their research area and chose a 10,702 m^2 concrete–CLT hybrid commercial building as the study object, reporting an average 26.5% reduction in global warming potential (GWP) relative to a conventional Ref. [22]. A notable feature of this region is the significantly higher number of large-scale multi-family buildings with mass timber as the main load-bearing structure. In Puettmann et al.'s study, three mixed-use buildings located in the Pacific Northwest, Northeast, and Southeast with areas of 9480 m^2, 14,220 m^2, and 21,330 m^2 were selected, underscoring that North America is among the most active regions in applying mass timber in large-scale commercial buildings [23]. It is worth noting that South American countries like Chile also have mass timber applications: Felmer et al. studied a 150 m^2 building in central Chile designed with Solar Decathlon strategies and observed roughly a one-third reduction in CO_2e per m^2 over 50 years compared with an equivalent concrete building [9]. Methodologically, these North American cases often focus on larger multi-family or mixed-use programs and adopt like-for-like assumptions (e.g., common envelope/MEP and declared A-modules), with recent code developments (e.g., IBC 2021 Type IV-A/B/C) enabling higher-rise prototypes that make system-level comparisons more representative at scale. Despite the availability of completed projects, A5 is still typically reported as a fixed share rather than inventoried at activity level.

The Oceania region has relatively fewer studies compared to other regions; nevertheless, the cross-climate evidence is valuable. Jayalath et al. compared reinforced-concrete and CLT buildings across Melbourne, Sydney, and Brisbane over a 50-year life span and found an average 31% lower GWP for mass timber buildings [5]. Lu et al. evaluated a four-storey apartment building in Brisbane and quantified both environmental (GWP, human-toxicity potential) and economic (life-cycle cost) outcomes for engineered-wood structural products, finding less than one-quarter of the emissions relative to an equivalent concrete frame while documenting

 Case Studies in Construction Materials 25 (2026) e06280

methods transparently (functional unit restricted to the structural frame, quantity-takeoff-based inventories, explicit LCC parameters and uncertainty analysis) [24]. These studies provide whole-building benchmarks but do not isolate A5.

In the Asia-Pacific region (China, Japan), there is a rich historical experience with wooden structures. Following late-twentieth-century concrete dominance, renewed decarbonization efforts have refocused attention on mass timber, especially in multi-family buildings. Liu et al. examined CLT substitution for concrete in cold-region mid-rise residential buildings (Xi'an and Harbin) and found >30% energy savings and >40% CO_2 reductions in both cities [25]. Nakano measured a CLT dwelling in Kyushu using delivered-fuel and metered-electricity data, providing rare, measured inputs that strengthen validation relative to plan-based studies [26]. Complementary regional standards (e.g., JAS-CLT) and technical guidelines are also expanding, which supports consistent data capture for A-modules and enables more comparable treatment of the A5 construction stage. Even so, activity-level A5 inventories for large-scale mass timber buildings remain rare here.

From the studies reviewed above, despite the growing number of LCA studies assessing the global-warming potential (GWP) of mass timber buildings, several common limitations persist. First, at the whole-building level, certain life-cycle stages, especially the A5 on-site construction stage, are sometimes treated as minor (e.g., approximated as ~3% of primary energy) and therefore reported at coarser resolution rather than explicitly inventoried; some studies even estimate A5 by multiplying other stages by a fixed percentage [27]. Specifically, prior LCA studies of mass timber buildings differ in three ways with respect to A5: (i) excluding A5 from the system boundary entirely; (ii) including A5 but approximating it as a fixed percentage of total embodied energy due to limited site data; or (iii) including A5 with activity-level inventories but under different system boundary assumptions. These differences reflect the varying scope of those studies rather than inaccuracy in their estimations. Second, sample sizes are often small: many studies examine a single building or compare only two to three buildings of similar scale but different structural systems (e.g., CLT vs. RC). Small samples limit statistical power and external validity and can yield results that are sensitive to case selection, while limited access to construction and operational records forces reliance on assumptions [28]. Third, most studies concentrate on smaller projects frequently single-family or small commercial while few cases exceed 1000 m^2; in our review, the mean floor area is 3722 m^2 and the median is 2012 m^2, which skews comparisons toward small-scale building types. Fourth, system boundaries remain inconsistent: many European studies emphasize the superstructure and exclude substructure (foundations), whereas parts of the Asia-Pacific literature include both, and data-quality declarations (e.g., region/year of emission factors and alignment with pre- vs. post-A2 EN 15804 datasets) are not always transparent, creating biases in cross-regional comparisons.

Taken together, these limitations point to a specific research gap: the lack of detailed, activity-based A5 inventories for large-scale mass timber construction, particularly in cold-climate regions. To address this gap, this study develops a dual-track framework for estimating A5 energy use in podium-supported multi-family buildings constructed with mass timber, structural steel, and reinforced concrete. The framework defines the A5 system boundary and functional unit (MJ/m^2), establishes a theoretical lower bound and a schedule-based upper bound, and incorporates floor-repetitive Monte Carlo simulation with learning-curve effects to characterize uncertainty. Using construction data from two completed mass timber buildings, INTRO and Ascent, the study quantifies A5 energy use by construction component, identifies the dominant drivers, and develops functionally equivalent reinforced concrete (RC) and structural steel options for Ascent to demonstrate cross-system applicability. External validation is conducted using Bakers Place, another completed mass timber project, a 14-story hybrid building for which four professionally designed structural schemes were available to assess the transferability of the proposed methodology. It should be noted that this study employs the A5 module solely to characterize construction phase energy use rather than executing a full LCA for the cases. However, this demonstrates that the proposed framework has the potential to be nested within comprehensive whole-building LCA tools.

2. Materials and methods

2.1. Study overview and system boundary

2.1.1. Functional unit and scope

This study develops an A5 life-cycle inventory (LCI) model to quantify on-site energy use during building construction, consistent with the LCA framework established by ISO 14040 and ISO 14044 and with life-cycle module definitions following ISO 21930 [29–31]. The functional unit is defined as construction energy use per square meter of gross floor area at substantial completion (MJ/m^2). Primary inputs are obtained from design drawings and project schedules/logs and are supplemented by manufacturer handbooks and industry databases. The transferability of the proposed framework is evaluated through an external case study using design-team-issued drawings and material quantity takeoffs from functionally equivalent structural schemes, including mass timber, reinforced concrete (RC), and structural steel.

2.1.2. A5 system boundary definition

The system boundary defines the life cycle stages and activities included in the analysis. This study focuses on the Construction Stage (A5), which starts when materials arrive at the construction site and includes all relevant activities until building completion and commission.

The A5 system boundary specifically includes on-site fuel and electricity consumption for construction equipment and temporary facilities (e.g., site offices and temporary heating systems), on-site transport and handling of materials and waste, temporary work and formwork turnover, and waste generation and management. To address potential ambiguities at the boundary, the following itemized treatment is applied consistently across all case studies: *included* on-site equipment fuel use, temporary heating and lighting (including site offices), temporary works and formwork turnover, and on-site material/waste transport and handling; *excluded* –

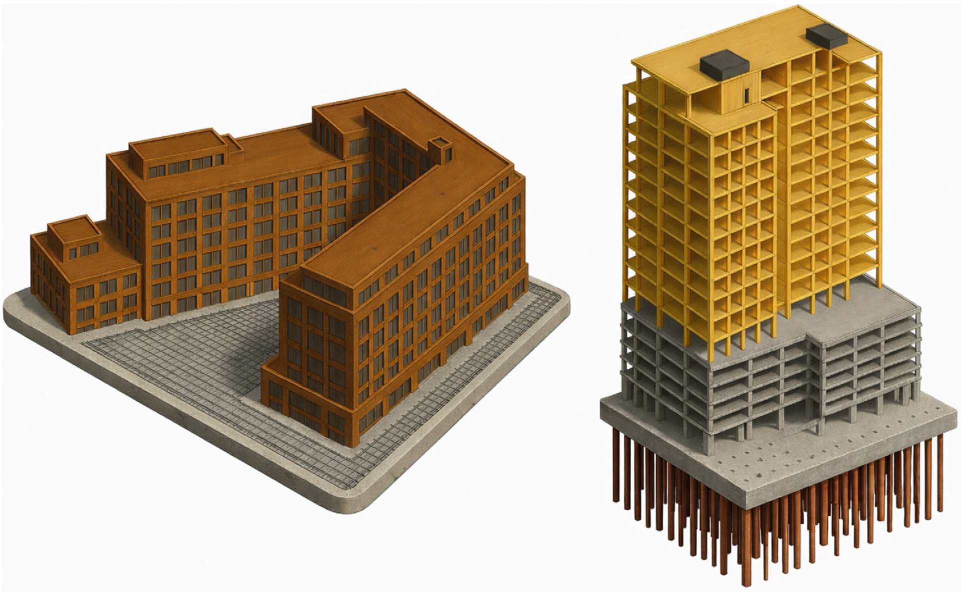

Fig. 1. Schematic diagram of two reference mass timber buildings (Left: INTRO; Right: Ascent).
Note: Renderings prepared by the authors based on architectural drawings provided by the design team.

worker commute (outside the on-site A5 boundary defined by ISO 21930, although reported as non-negligible in some studies), off-site packaging, and small hand-tool battery charging (the latter two each estimated to contribute less than 1% of A5 energy). For comparison, the proposed ASHRAE/ICC Standard 240P [32] further subdivides the Construction & Installation stage into A5-1 (pre-construction demolition), A5-2 (on-site construction activities), and A5-3 (construction waste processing and disposal). A5-1 (pre-construction demolition) is highly project-specific and therefore not explicitly modeled. A5-3 (construction waste processing and disposal) is incorporated as supporting reference data to maintain completeness of the construction-stage boundary, while detailed analysis focuses on A5-2. The environmental impacts during construction extend beyond energy consumption. Emissions and environmental burdens from dust, noise, and wastewater during construction contribute significantly to the overall life cycle impact of a building. These non-energy impacts are acknowledged but are not included in the present framework, which focuses exclusively on A5 energy quantification; other ISO 21930 modules (A1–A3, A4, B, C, D) are outside scope and are addressed in dedicated whole-building LCA tools.

2.1.3. Building model assumptions

For model simplicity, the present A5 inventory includes only load-bearing components. Non-load-bearing items—cladding, interior partitions, finishes, insulation, bathroom fixtures, and MEP systems—are excluded identically across mass timber, RC, and steel options, so they do not contribute to the cross-system A5 differences quantified in this study.

2.2. Case study buildings

2.2.1. Reference mass timber buildings

The reference mass timber buildings for this study are two multi-family projects used to develop the model. The first is a 9-story, 54-meter-tall building (INTRO) located in Cleveland, with a total gross area of 60,666 m^2. The lower two stories are designated for commercial use, including underground parking and rental shops. The remaining floors are residential units constructed with all load-bearing beams, slabs, and columns made of mass timber.

The second building (Ascent) is located in Milwaukee, Wisconsin. The Ascent structure is composed of 7 levels of parking podium, with 18 stories of residential units, standing 87 m tall, with a total gross floor area of 45,838 m^2. The podium was built with reinforced concrete columns and post-tension flat slabs. The mass timber superstructure comprises glulam beams and columns and CLT slabs. The key structural difference between the Ascent and INTRO is the use of a raft foundation in Cleveland versus pile foundations in Milwaukee, reflecting differing vertical and horizontal load demands. Fig. 1 provides a conceptual representation of the buildings.

Field data for the two reference projects were obtained through direct collaboration with the project contractors (Panzica Construction for INTRO and C.D. Smith for Ascent). The daily equipment logs, monthly progress schedules, and equipment-hour records covering the full A5 period were generated by the contractors as part of their routine project management activities and subsequently shared with the research team. The records were cross-verified against design drawings and project schedules, then processed by the lead author into the activity-level A5 inventory used throughout this study.

2.2.2. Functionally equivalent options

To enable comparative analysis of A5 energy across structural systems, functionally equivalent reinforced concrete (RC) and structural steel options are designed for comparison with the mass timber building following the dual-track methodology described in Section 2.3. All options maintain identical gross floor area, building height, functional program, and core/foundation configuration, differing only in the superstructure material system.

Due to the lighter weight of timber materials, foundation requirements differ significantly across structural systems. Although site-specific variations in soil conditions exist between Milwaukee and Cleveland, this study standardized foundation type selection based on the primary load characteristics (horizontal and vertical) sustained by each building. Because the upper structure is made of timber, the excavation volume and foundation construction quantity in the deep foundation portion are significantly lower than those of traditional reinforced concrete buildings. Chan pointed out that a 14-story mass timber building weighs almost half as much as an equivalent reinforced concrete structure [33]. This weight differential forms the basis for the option assumptions described below.

Reinforced concrete option. The deep foundation concrete volume for the RC option is set at 2.0 times the mass timber baseline. This ratio is supported by converging evidence from the structural engineering literature, indicating that the structural self-weight of mid- to high-rise mass timber buildings is approximately 45%–55% of an equivalent RC structure [33], requiring RC foundations to resist approximately twice the vertical load, with foundation volumes scaling accordingly. Hassan et al. compared glulam and RC columns designed to identical loading conditions under Eurocode 2 and 5, confirming that while RC members can achieve comparable load capacity, the resulting member weight is substantially greater—at the individual member level, glulam structural elements weigh approximately one-sixth as much as equivalent RC members for the same load capacity [34]. The whole-building self-weight ratio (45%–55%) is less extreme than this member-level ratio because mass timber buildings still rely on concrete cores, podiums, and floor toppings. This strength-to-weight disparity means that achieving equivalent structural performance in RC requires larger and heavier members, compounding foundation demands. This assumption is independently corroborated by the Bakers Place structural quantity data (Table 6), where the RC foundation concrete volume (1518 m^3) is 2.0× the mass timber baseline (759 m^3).

For the superstructure, all timber columns, beams, and floor systems are replaced with cast-in-place RC elements. Member dimensions are determined following the principle of equivalent load capacity and deflection control: because RC members exhibit lower strength-to-weight ratios than timber–steel hybrid systems, larger cross-sections and thicker floor slabs are required to satisfy the same structural performance requirements [34]. Overall, the total superstructure concrete volume for the RC option is substantially greater than the mass timber baseline, reflecting cumulative increases across columns, beams, floor slabs, and shear walls. The increase in concrete volume also results in extended formwork turnover cycles and longer curing periods, which are accounted for in the schedule-based track through an extended construction duration of 26 months for RC, compared to 20 months for the mass timber system.

Structural steel option. The deep foundation concrete volume for the steel option is set at 1.5 times the mass timber baseline. Although steel has a higher unit density than concrete, the sectional efficiency of steel members is significantly greater than that of RC, yielding an overall structural self-weight intermediate between mass timber and reinforced concrete—well below an equivalent RC system but above mass timber [34]. Accordingly, the foundation load increment is smaller than that of the RC option.

For the superstructure, all timber columns and beams are replaced with wide-flange steel sections, with member sizes selected based on equivalent load capacity and deflection control requirements. The floor system employs steel decking with lightweight concrete topping, following standard North American practice. The concrete core and podium configuration remain unchanged from the mass timber baseline, ensuring functional equivalence in the comparative analysis.

Regarding construction duration, unlike the RC option, where schedule extension is driven by curing and formwork constraints, the steel option schedule is governed by on-site erection rates. RSMeans productivity data indicate that steel decking installation requires approximately 0.008 man-hours per square foot [35]. Field data from the INTRO project yield mass timber floor installation rates of 0.006 man-hours per square foot during early phases, improving to 0.0045 man-hours per square foot during later phases due to learning curve effects (see Section 3.1.4). Comparing against the early-phase timber rate, steel erection requires approximately 33% more labor time per unit area; comparing against the project-average rate (~0.005 man-hours per square foot), the differential widens to approximately 60%. This productivity differential is applied to the superstructure installation phase, resulting in a moderately extended overall construction duration relative to mass timber.

2.3. Dual-track calculation framework

Existing studies have employed various methods to estimate energy use in the A5 (building construction) stage. Gustavsson approximated A5 as a fixed percentage of total energy [27]; Tettey split A5 evenly between diesel and electricity [36]; Liu used regressions calibrated to Athena empirical data to estimate task-level energy [25]; and Nakano directly metered site electricity in several cases [26]. From these examples, we observe that although many studies draw substantially on databases, few isolate A5 as a dedicated target, and most rely on broad assumptions while omitting quantitative detail. This study develops a reference-data-based framework to fill the gap.

The A5 stage energy components included in our proposed framework are illustrated in Fig. 2. This study employs a dual-track methodology to quantify A5 energy use. The theoretical track establishes a deterministic lower bound by multiplying quantity takeoffs by the unit energy coefficients. This addresses the question of "what is the minimum energy required theoretically?" The practical track establishes a probabilistic upper bound by using actual equipment times from project logs, accounting for real-world inefficiencies such as equipment idling, weather delays, and coordination losses. This addresses the question of "what energy is likely consumed under realistic conditions?"

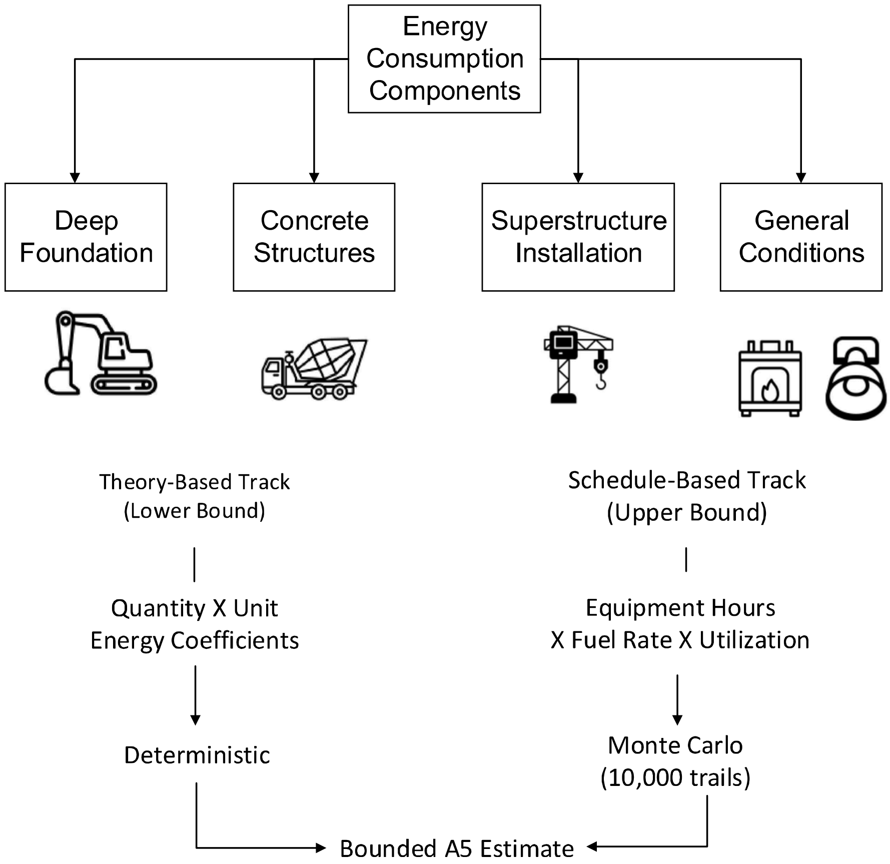

Fig. 2. A5 energy consumption analysis framework.

2.3.1. *Theoretical track (lower bound)*

The theory-based track calculates energy consumption by multiplying the quantity of each construction operation (e.g., cubic meters of concrete, tons of steel lifted) by declared unit energy coefficients and then normalizing the results per unit of gross floor area. This approach assumes ideal sequencing, minimal equipment idling, and optimal crew coordination. Because it excludes real-world inefficiencies, the result represents a calculated lower bound. Specific unit coefficients for each construction component are presented in Section 2.4.

2.3.2. *Practical track (upper bound)*

The schedule-based track derives energy consumption from logged equipment operating hours and manufacturer-specified fuel or power consumption rates. Unlike the theory-based track, this approach explicitly accounts for equipment utilization (the fraction of time under productive load versus idling) and production rate variability due to weather, traffic, and crew coordination. For diesel equipment, fuel consumption combines productive-load consumption and idle consumption weighted by the utilization factor. For electric equipment such as tower cranes, electricity consumption similarly combines full-load and idle power draw, adjusted by a motion factor reflecting actual hoist/travel activity.

Monte Carlo simulation (10,000 trials per building) is applied to propagate uncertainty from two independent sources. The first set of parameters governs equipment operations on the schedule-based track: utilization factor, idle ratio, and production rate variability, with distributions calibrated against field logs and published benchmarks [37,38]. Crucially, the weather delay factor is explicitly parameterized as an asymmetric triangular distribution, expressed as Triangular($\text{Min} = 1.0, \text{Mode} = 1.0, \text{Max} = 1.3$), calibrated to localized climate historical data [39]. The second set governs temporary heating in the general conditions component (Eq. (1)): envelope tightness $F_{tightness}$, heater duty cycle F_{load}, and heating-period duration driven by heating degree days (HDD), as introduced in Section 2.4. A sanity check confirms that under baseline values (Milwaukee, 5A) the Monte Carlo mean of the heating sub-model recovers the deterministic Rankin Group estimate to within 0.1%, validating the parameterization. Results across both tracks are reported as the median (point estimate) and 5th–95th percentiles (90% credible interval). The complete parameter set is summarized in Table 1.

Table 1
Monte Carlo simulation parameters.

Parameter	Distribution	Range	Source
Schedule-based track (equipment operations)			
Utilization factor (η)	Triangular	0.60–0.85	Lewis et al. [37]; Field logs
Idle ratio (r)	Uniform	0.25–0.40	Lewis et al. [37]
Production rate variability	Log-normal	CV = 0.15	AbouRizk et al. [38]
Weather delay factor	Triangular	1.0, 1.0, 1.3	Milwaukee/Cleveland climate [39]
Heating sub-model (general conditions, Eq. (1))			
Envelope tightness ($F_{tightness}$)	Triangular	1.5–2.5 (mode 2.0)	Tarp-enclosure field range
Heater duty cycle (F_{load})	Uniform	0.4–0.6	Day/night cycling
HDD variability	Normal	CV = 10%	NOAA TMY3 inter-annual
Number of trials	–	10,000	–

2.4. Component-specific energy models

This section presents the energy calculation methods for each structural component. Fig. 2 illustrates the coordination of construction equipment across project phases.

2.4.1. Deep foundation

This study quantifies the A5 energy for two foundation systems: raft foundations (INTRO) and pile foundations (Ascent). Raft foundations concentrate energy in earthwork operations, with unit coefficients of 0.79 L/m^3 for excavation, 0.20 L/m^3 for transportation/haul, 0.10 L/m^3 for leveling, and 0.40 L/m^3 for backfilling. For pile foundations, a composite coefficient of 1.68 L/m^3 reflects combined piling and pile cap construction activities. These coefficients are derived from the contractors' fuel records and equipment manufacturer specifications.

For schedule-based calculations, logged equipment hours from the project records are combined with manufacturer fuel consumption specifications. The primary equipment are the Cat 385C MH for earthwork and material handling and the Link-Belt TCC-1100 telescopic crawler crane for driving piles. When logs provide separate auxiliary equipment hours, auxiliaries are modeled explicitly; otherwise, a fixed share of primary equipment energy is applied.

2.4.2. Concrete structures

Concrete placement energy includes pumping, placing, vibration/finishing, and associated support for all concrete elements: foundations, cores, slabs, walls, and columns. Unit energy coefficients are differentiated by element type, with heavily reinforced core elements assigned higher coefficients than general slabs and walls. A height multiplier derived from manufacturer pump curves is applied to reflect additional pumping effort at elevation.

Schedule-based calculations use logged pour durations and manufacturer fuel consumption specifications for the Putzmeister BSA 14000 pump, placing boom, vibrators, and auxiliaries. For floor-by-floor pours, cycle times incorporate learning effects; deep-foundation pours use recorded durations without learning adjustments. Fuel is converted to MJ using the lower heating value of 35.8 MJ/L for diesel; all reported MJ values throughout this study represent final (delivered) energy on site—that is, the lower heating value of fuel delivered to the site, and electricity at 3.6 MJ/kWh—and do not include upstream extraction, refining, or transmission losses.

2.4.3. Superstructure installation

For mass timber installation, the theory-based track computes the gravitational potential energy required to elevate timber components from ground level to installation height. The schedule-based track uses logged equipment times for the Liebherr 316 EC-H electric tower crane and diesel telehandlers, with utilization factors and motion factors applied per Table 1.

A distinctive aspect of timber construction is mechanical fastener installation. Based on torque-rotation testing [40], a typical 400 mm self-tapping screw consumes approximately 14,360 J. Total fastener quantities were estimated by multiplying the standard screw count per connection type (e.g., floor-to-beam, column-to-beam) by the number of corresponding structural components identified in the design drawings. For the Ascent (280,000 screws) and INTRO (120,000 screws), cumulative fastener energies equal approximately 4.0 GJ and 1.7 GJ, respectively—equivalent to 0.03–0.09 MJ/m^2, representing less than 0.2% of total installation energy. This value reflects the mechanical work to drive screws (torque × angular displacement); associated overheads such as battery charging, tool standby losses, and access-equipment time are captured implicitly through the broader timber-installation track via equipment-hour logs. This finding demonstrates that fastener work does not constitute a significant energy component in mass timber construction.

The second installation activity specific to mass timber is gypsum board encapsulation for fire protection, which is not required for the RC or structural steel options. Based on drywall installation productivity data [35], this activity is estimated to contribute on the order of a few percent of total A5 energy in mass timber projects.

Table 2
Summary of key calculation parameters.

Component	Parameter	Value	Unit
Deep foundation (raft)	Excavation coefficient	0.79	L/m^3
Deep foundation (raft)	Haul coefficient	0.2	L/m^3
Deep foundation (raft)	Leveling coefficient	0.1	L/m^3
Deep foundation (raft)	Backfill coefficient	0.4	L/m^3
Deep foundation (pile)	Composite coefficient	1.68	L/m^3
Concrete	Diesel lower heating value	35.8	MJ/L
Timber installation	Fastener energy	14,360	J/screw
General conditions	Envelope tightness factor	1.5–2.5 (mode 2.0)	–
General conditions	Heating duty cycle	0.4–0.6	–
General conditions	Propane calorific value	25.6	MJ/L
Option assumptions	RC foundation multiplier	2	–
Option assumptions	Steel foundation multiplier	1.5	–

Note: Foundation coefficients derived from the contractor fuel records. Fastener energy based on Zhang et al. [40]. General conditions parameters from Rankin Group specifications. Option multipliers based on Chan [33] and converging structural engineering literature.

2.4.4. General conditions

General conditions encompass support activities critical for construction progress. In cold climate regions, temporary heating and lighting dominate this category.

Lighting energy is calculated using RSMeans [35] temporary utility methodology, considering building area, construction duration, and geographic location factors. Temporary heating energy demand was estimated using a methodology developed by the climate control provider Rankin Group. The propane consumption is calculated as:

$$Q_{fuel} = \frac{A_{deck} \times H_{floor} \times F_{tightness}}{100,000} \times F_{load} \times 24 \times D_{heating} \tag{1}$$

where Q_{fuel} is propane consumption (gallons), A_{deck} is the actively enclosed deck area (sq ft), H_{floor} is the floor-to-floor height (ft), $F_{tightness}$ is the envelope tightness factor (dimensionless, characterizing temporary enclosure quality), F_{load} is the heater duty cycle (dimensionless), and $D_{heating}$ is the heating-period duration (days) determined by topping-out date and local heating degree day (HDD) climatology. The calculation is performed in imperial units (consistent with industry practice for this empirical formulation) and the result is converted to MJ to align with the functional unit adopted throughout this study (note: 1 m^2 = 10.764 sq ft; 1 m = 3.281 ft; propane converted at 3.785 L/gal and 25.6 MJ/L).

To quantify uncertainty in heating energy, the three parameters are treated as random variables in the Monte Carlo framework (Section 2.3.2): $F_{tightness} \sim \text{Triangular}(1.5, 2.0, 2.5)$ spanning tight to leaky tarp enclosures with central value 2.0; $F_{load} \sim \text{Uniform}(0.4, 0.6)$ reflecting day-night and weather-driven cycling; and $D_{heating}$ scales with HDD $\sim \text{Normal}(\text{HDD}_{\text{city}}, \text{CV} = 10\%)$ to capture year-to-year climate variability. Propane consumption is converted to MJ using a calorific value of 25.6 MJ/L. Section 3.4 extends this framework across ASHRAE Climate Zones 5A through 1A. It should be noted that this framework was developed and calibrated using projects in ASHRAE Climate Zone 5A; although Section 3.4 validates its extension to warmer zones, the general-conditions composition characterized here may not apply uniformly to mild, warm, or tropical climates.

2.5. Summary of key parameters

Table 2 summarizes all key parameters used in the dual-track methodology calculations. These values derive from published benchmarks, manufacturer specifications, field observations, and standard energy conversion factors.

3. Results

Construction-stage (A5) energy remains one of the least quantified phases in building life cycle assessment, and current practice often relies on simplified assumptions that may significantly underestimate actual energy consumption. Results from this study indicate that A5 energy intensities are two to three times higher than values commonly assumed in the literature, underscoring the need for systematic, component-level quantification. The dual-track framework developed in this study addresses this gap by producing bounded energy estimates theoretical lower bounds and schedule-based upper bounds for mass timber, reinforced concrete, and structural steel systems.

3.1. A5 energy intensities for mass timber buildings

3.1.1. Overview of dual-track estimates

Table 3 presents the A5 construction energy intensities for mass timber buildings derived from the dual-track methodology. The theory-based approach yields a lower-bound estimate of 156.0 MJ/m^2, while the schedule-based approach produces a Monte Carlo median of 166.3 MJ/m^2 with a 90% credible interval of 139.4–198.5 MJ/m^2.

Table 3
A5 construction phase energy intensities (MJ/m^2 gross floor area).

Component	Theory-based (lower bound)	Schedule-based (upper bound)
Deep foundation	16.3	31.1
Concrete structures	12.9	13.0
Timber installation	33.7	41.1
General conditions	93.1	123.1
Total (MC range)	139.4	198.5

Note: The Theory-based value for “General conditions” corresponds to the central deterministic case of Eq. (1) ($F_{tightness}$ = 2.0, F_{load} = 0.5, baseline HDD); the Schedule-based value reflects the 95th-percentile upper bound when these three parameters are propagated through the Monte Carlo framework introduced in Section 2.3.2 (parameters in Table 1).

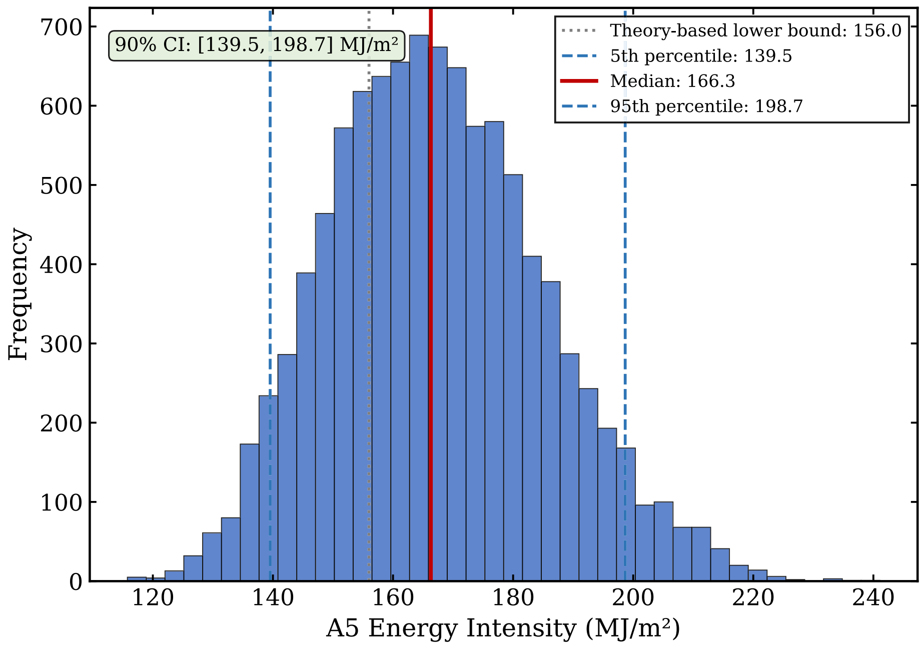

Fig. 3. Monte Carlo distribution of A5 energy intensity.

3.1.2. Uncertainty quantification via Monte Carlo simulation

To characterize the uncertainty inherent in construction-stage energy estimation, Monte Carlo simulation (n = 10,000) was performed using the schedule-based parameters. Fig. 3 presents the resulting probability distribution of total A5 energy intensity.

The simulation yields a median estimate of 166.3 MJ/m^2 with a 90% credible interval (5th–95th percentile) of 139.4–198.5 MJ/m^2. The median is adopted as the schedule-based point estimate because it is robust to outlying simulation trials and provides a more representative central tendency than the arithmetic mean. The full predicted range for the dual-track methodology is therefore bounded by the 5th-percentile (139.4 MJ/m^2) and the 95th-percentile (198.5 MJ/m^2) of the Monte Carlo distribution, characterizing propagated uncertainty across all four components (deep foundation, concrete structures, timber installation, and general conditions).

The relative influence of each stochastic parameter on simulation variance can be inferred from the dual-track structure. Among the schedule-based track parameters, the weather delay factor exerts the largest influence on simulation variance because it simultaneously scales equipment operating hours across all construction components. The utilization factor has a moderate effect concentrated in foundation and installation operations, while production rate variability and idle ratio contribute comparatively less variance. The heating sub-model parameters ($F_{tightness}$, F_{load}, and HDD variability) jointly drive the broader credible interval observed in Fig. 3, reflecting the dominant share of general-conditions energy in cold-climate A5 totals.

3.1.3. Component breakdown and key findings

Analysis of the component-level energy breakdown reveals several important findings with implications for construction practice.

In cold-climate projects, temporary heating dominates A5 energy consumption. General conditions — primarily temporary heating — account for 52%–60% of total A5 energy, representing the single largest contributor. This finding suggests that strategic scheduling to avoid winter construction periods offers greater A5 energy reduction potential than optimizing any individual

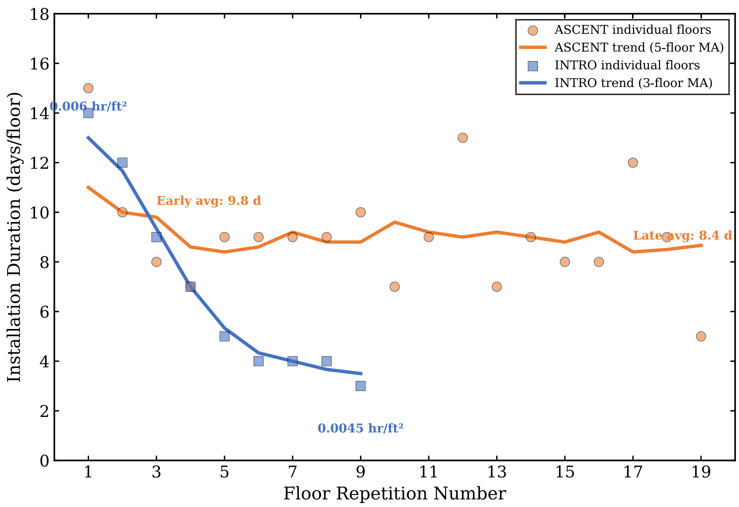

Fig. 4. Learning curve for CLT panel installation productivity across floor repetitions.

construction operation. For cold-climate projects, compressing the construction schedule to span a single winter rather than two could reduce total A5 energy by 25–30%—a benefit far exceeding what is achievable through equipment efficiency improvements alone.

Timber installation plays the second-largest energy contributor as a component, representing 20%–23% of total A5 energy (33.7–41.1 MJ/m^2). Within timber installation, vertical transport operations — tower crane lifting CLT panels, glulam beams, and columns — dominate the energy consumption. This indicates that crane selection and lift optimization represent the highest-leverage opportunities for reducing timber installation energy. Notably, although some studies have identified mechanical fastener installation as a potentially significant energy component unique to mass timber construction, the present analysis found fastener energy consumption of only 0.03–0.09 MJ/m^2—less than 0.2% of total timber installation energy. This finding demonstrates that fastener work does not constitute a meaningful barrier to achieving high energy efficiency in mass timber construction, and concerns about fastener-related energy penalties appear overstated in the literature.

Concrete structure energy exhibits strong convergence between theory-based and schedule-based estimates (12.9–13.0 MJ/m^2), reflecting the mature and predictable nature of concrete pumping operations. This tight convergence provides confidence in the modeling approach and suggests that concrete placement energy can be reliably estimated from material quantities alone in future studies. Deep foundation energy displays wider variability (16.3–31.1 MJ/m^2), reflecting differences between raft foundation and pile foundation configurations evaluated during model development. The schedule-based upper bound captures the additional energy associated with such activities as extended excavation time, soil stabilization requirements, and equipment idle time during geotechnical inspections.

These findings reveal building height as a compounding driver of A5 energy intensity. Taller buildings typically require pile foundations rather than raft foundations (increasing foundation energy by 50%–90%) and demand more vertical lift work against gravity (increasing installation energy proportionally with height). These interdependencies suggest that A5 energy does not scale linearly with floor area but exhibits a height premium that merits explicit consideration in early-stage design decisions.

3.1.4. Learning curve effects in timber installation

Field construction logs from the two projects revealed pronounced learning-curve effects in repetitive timber installation work, representing a novel quantitative finding with significant implications for construction planning and energy forecasting. Fig. 4 presents the observed learning curve for CLT panel installation productivity across floor repetitions.

The schedule-based track incorporates a learning curve [41] to represent productivity improvement across floor repetitions, expressed as:

$$T_n = T_1 \cdot n^{-b} \tag{2}$$

where T_n is the unit labor time for the nth repetition, T_1 is the initial unit labor time, and b is the learning coefficient. A learning coefficient of $b = 0.15$ was adopted based on Mirando and Onsarigo's [42] analysis of large-scale mass timber construction scheduling. This coefficient implies an approximately 10% reduction in unit labor time for each doubling of floor repetitions. The floor-by-floor field data from the Ascent project (Table 4 and Fig. 4) provide independent empirical validation of this coefficient.

The data reveal that CLT panel installation productivity improved from 18 panels per day during early floors (L8–L12 in Ascent) to 26 panels per day during late floors (L20–L25)—a 44% efficiency gain. Correspondingly, mean per-floor installation time decreased from 9.8 days to 7.1 days, representing an approximately 28% reduction in installation duration between early and late construction phases.

Table 4
CLT installation productivity by construction phase.

Phase	Mean duration (days/floor)	Productivity (panels/day)	Cumulative improvement
Early	9.8	18	Baseline
Middle	9.4	22	+22%
Late	7.1	26	+44%

Table 5
Comparative A5 energy intensities across three structural systems (MJ/m^2 GFA).

Component	Mass timber		Reinforced concrete		Structural steel	
	Theory	Schedule	Theory	Schedule	Theory	Schedule
Deep foundation	16.3	31.1	32.6	62.2	24.5	46.7
Concrete structures	12.9	13.0	68.9	69.0	22.6	25.4
Superstructure installation	33.7	41.1	–	–	26.2	33.5
General conditions	93.1	123.1	121.0	160.0	102.4	135.4
Total (90% CI)	139.4–198.5		200.7–278.6		160.5–226.7	
vs. Mass timber	Baseline		+42%		+15%	

Note: For the RC option, superstructure construction energy is included in *Concrete structures*, as cast-in-place operations are inseparable from concrete placement.

The productivity improvement translates to energy savings of 8–12 MJ/m^2 relative to a constant-productivity baseline assumption. Specifically, if late-floor productivity (26 panels/day) had been achieved from project inception, total timber installation energy would have decreased by approximately 25%. This finding indicates substantial optimization potential for contractors executing multiple mass timber projects or projects with significant floor repetition.

The convergence of shortened installation duration with reduced temporary heating requirements creates a compounding benefit: faster timber installation not only reduces crane and equipment energy directly but also compresses the overall construction schedule, thereby reducing the duration of temporary heating demand—the largest single A5 energy contributor.

3.2. Cross-system comparison

Based on the functional equivalence assumptions established in Section 2.2.2, A5 energy consumption for alternative structural systems (reinforced concrete and structural steel) was calculated following the dual-track modeling framework. Table 5 presents the comparative results.

Fig. 5 illustrates the component-level energy breakdown across the three structural systems, enabling visual comparison of the drivers underlying cross-system differences.

3.2.1. Reinforced concrete

The reinforced concrete option exhibits approximately 42% higher A5 energy than mass timber (median: 235.9 vs. 166.3 MJ/m^2). This substantial difference stems from compounding effects across all construction phases. Unlike mass timber buildings, where concrete work is confined primarily to foundations and floor toppings, RC buildings require cast-in-place concrete for the entire superstructure—slabs, beams, columns, and shear walls.

While excavation volume remains largely determined by functional basement requirements, the heavier RC superstructure imposes substantially greater foundation demand — manifested either as deeper piling or as thicker raft foundations. The present cross-system comparison adopts the Ascent-based pile-foundation configuration (Section 2.2.2) for all three structural systems, yielding a 50%–80% increase in foundation energy for the RC option relative to mass timber.

Concrete structure energy increases from 12.9–13.0 MJ/m^2 (mass timber) to 68.9–69.0 MJ/m^2 (RC). The heavier structural system also demands larger load-bearing member dimensions and thicker floor slabs to satisfy deflection control requirements, further amplifying placement energy. This fundamental difference in construction logic — localized concrete use versus whole-building casting — accounts for the majority of the A5 energy penalty.

General conditions energy increases by 28 MJ/m^2 (from 93.1 to 121.0 MJ/m^2), driven by construction schedule extension from 20 months (mass timber) to 26 months (RC). This 30% schedule increase results from concrete curing time requirements and formwork turnover limitations inherent to cast-in-place construction. Critically, the extended schedule introduces an additional partial winter heating season, raising temporary heating energy proportionally (93.1 → 121.0 MJ/m^2, a 30% increase)—a major driver of the dominant A5 component.

3.2.2. Structural steel

Foundation energy increases by approximately 15 MJ/m^2 relative to mass timber. Due to its greater self-weight, deep foundation volumes and concrete placement for the steel system are scaled to 1.5 times the timber baseline, resulting in a proportional increase in foundation energy. Steel superstructure installation energy (26.2–33.5 MJ/m^2) falls below timber installation energy

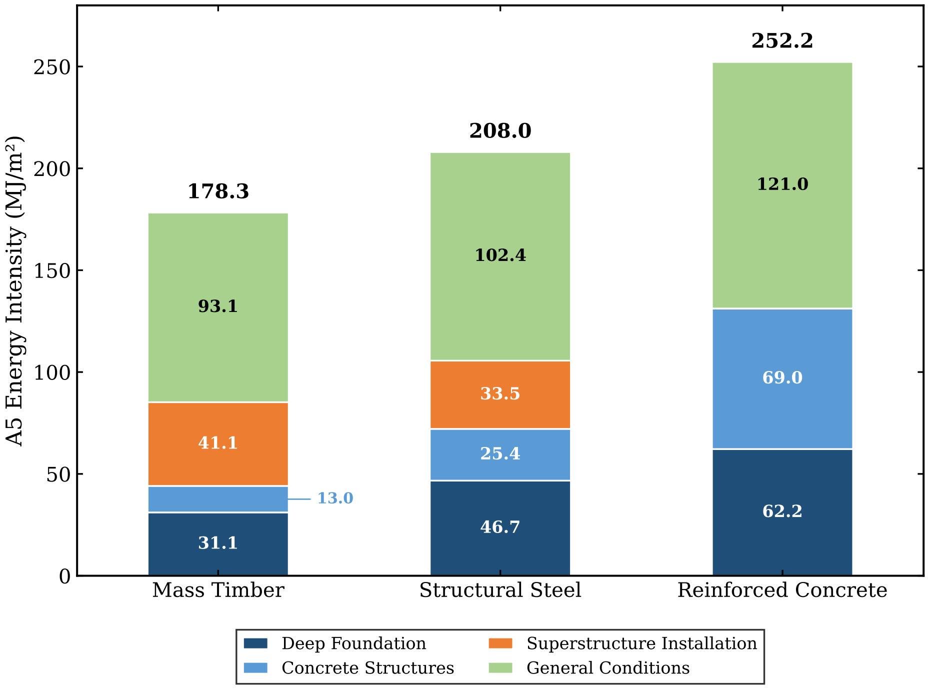

Fig. 5. A5 energy breakdown by structural system, presented as a stacked bar chart. The results illustrate the relative contribution of major construction-stage energy components across mass timber, structural steel, and reinforced concrete systems.

(33.7–41.1 MJ/m^2), as steel erection requires fewer crane picks and faster bolted connections than the multi-fastener assemblies typical of timber construction.

However, the steel system does not achieve the same construction duration as mass timber, despite the faster erection speed of steel members. RSMeans productivity data indicate that steel decking installation requires approximately 0.008 man-hours per square foot, compared to 0.006 man-hours per square foot for mass timber floor systems [35]—a ratio of approximately 1.33. When applied to the superstructure installation phase, which represents approximately 35% of total construction duration, the overall project schedule extends by approximately 10%, from 20 months to approximately 22 months. This schedule extension increases general conditions energy from 93.1 to 102.4 MJ/m^2, driven primarily by additional temporary heating demand during the extended construction period.

As a result, the total A5 energy difference between structural steel and mass timber is approximately 15%, with steel exhibiting higher overall energy consumption (160.5–226.7 MJ/m^2 versus 139.4–198.5 MJ/m^2). While still substantially lower than the 42% penalty observed for reinforced concrete, the steel premium is larger than previously assumed under equal-duration assumptions. The primary drivers of the steel premium are increased foundation energy (due to higher structural weight) and extended general conditions (due to longer erection schedules), which together outweigh the efficiency advantages of steel superstructure installation.

For projects where foundation conditions are favorable or construction schedules are compressed through accelerated erection techniques, the A5 differential between timber and steel may narrow. Conversely, in cold-climate projects where temporary heating dominates general conditions energy, even modest schedule extensions can produce disproportionate A5 energy increases.

3.2.3. Supplementary CO_2e conversion

While the primary functional unit of this study is energy intensity (MJ/m^2), we provide an indicative carbon-equivalent conversion using published emission factors for each on-site energy carrier: 0.0749 kgCO_2e/MJ for diesel and 0.0590 for propane (U.S. EPA, 2024 [43]); and 0.117 kgCO_2e/MJ for U.S. average grid electricity (U.S. EPA eGRID 2023 [44]). Assuming representative fuel mixes by component (diesel-dominant for foundation, concrete, and steel/diesel installation; electricity-dominant for the tower crane in timber installation; propane-dominant for temporary heating), the schedule-based upper-bound A5 CO_2e intensities are approximately 13 kgCO_2e/m^2 for mass timber, 15 for structural steel, and 18 for reinforced concrete. These values are first-order estimates intended as a reference; energy intensity (MJ/m^2) remains the primary metric for cross-system comparison.

3.3. External validation: The bakers place case study

To validate the transferability and generalizability of the dual-track methodology, predicted energy ranges were compared against external benchmark data for the Bakers Place project, a 14-story mixed-use building built in Madison, Wisconsin in 2025.

Table 6
Material Quantities for the three equivalent structural systems designed for the bakers place [45].

Building section/material	Unit	Mass timber	Steel	Concrete
Floor and Roof				
Concrete	m^3	3 308	3308	5863
Concrete Benchmark USA 4000 psi	m^3	271	271	271
Concrete Benchmark USA 5000 psi	m^3	1 069	1603	2137
Lightweight Concrete	m^3	606	1210	0
Steel Reinforcement Rebar	Tonnes	197	210	426
Steel Deck (Galvanized Decking)	Tonnes	3	136	0
Cross Laminated Timber (CLT)	m^3	2 335	0	0
Steel Plate Connection	Tonnes	13	20	0
Gypsum Wall Board (GWB)	m^2	27 647	0	0
Foundation				
Concrete	m^3	759	1138	1518
Steel Reinforcement Rebar	Tonnes	19	79	38
Concrete Benchmark USA 4000 psi	m^3	219	285	340
Concrete Benchmark USA 5000 psi	m^3	0	0	41
Concrete Benchmark USA 6000 psi	m^3	0	0	112
Column and Beam				
Steel Reinforcement Rebar	Tonnes	39	51	68
Cold-formed Hollow Structural Steel	Tonnes	155	160	1
Hot-rolled Structural Steel	Tonnes	112	542	0
Spray Fireproofing	Tonnes	59	214	0
Glue Laminated Timber (GLT)	m^3	341	0	0
Steel Plate Connection	Tonnes	30	0	0
Wall				
Concrete	m^3	997	997	1458
Steel Reinforcement Rebar	Tonnes	119	119	173

Table 7
Bakers place A5 energy validation comparison (MJ/m^2 gross floor area).

Structural system	Predicted range	Designed [45]	Validation status
Structural steel	160.5–226.7	180.1	✓ Contained
Mass timber	139.4–198.5	173.0	✓ Contained
Reinforced concrete	200.7–278.6	220.9	✓ Contained

Note: Predicted ranges are derived from the dual-track methodology; LCA observations are from a previously conducted LCA assessment by the Bakers Place study team [45].

3.3.1. Validation approach

Bakers Place (Madison, Wisconsin) is a completed mass timber project that was *not* included in the framework calibration dataset (INTRO, Ascent), and therefore serves as a strictly external case at the building level—constructed by a different contractor team in a different city and completed in a different time period from the calibration buildings. The Bakers Place structural engineering team developed four functionally equivalent designs with mass timber and other options. The developers conducted the previously published whole-building LCA using tools such as Athena Impact Estimator and Tally [45]. The analysis included detailed quantity takeoffs (Table 6) and A5 energy estimates, providing external benchmark data for our methodology validation.

From Table 6, the foundation material quantities also follow the generally observed industry ratios: reinforced concrete (RC) construction requires approximately twice the foundation work of mass timber, while steel requires approximately 1.5×. This pattern aligns with the assumptions embedded in the dual-track model and provides confidence in the comparability of the validation cases.

The dual-track model was applied to the Bakers Place using project-specific parameters (climate zone, construction schedule, and material quantities), while maintaining the methodology structure developed from the INTRO and Ascent case studies.

3.3.2. Validation results

Table 7 presents the comparison between dual-track predictions and independent LCA observations.

All three structural systems validate successfully. For mass timber, the observed value (173.0 MJ/m^2) falls within the predicted 90% credible interval (139.4–198.5 MJ/m^2). For structural steel, the observed value (180.1 MJ/m^2) falls within the predicted interval (160.5–226.7 MJ/m^2). For reinforced concrete, the observed value (220.9 MJ/m^2) falls within the predicted interval (200.7–278.6 MJ/m^2). These results confirm that the dual-track methodology transfers effectively to independent projects with different scales, locations, and design teams.

3.3.3. Analysis of RC prediction range

The RC prediction interval (200.7–278.6 MJ/m^2) contains the observed Bakers Place value (220.9 MJ/m^2) comfortably. The 2.0× foundation multiplier adopted in Section 2.2.2 is independently corroborated by the foundation concrete ratio observed in the Bakers

Table 8
A5 energy intensities across ASHRAE climate zones (MJ/m^2, theory–schedule range).

City (Zone)	HDD	Mass timber	Reinforced concrete	Structural steel	MT vs. RC	MT vs. Steel
Milwaukee (5A)	7200	139.4–198.5	200.7–278.6	160.5–226.7	−29.5%	−12.9%
Baltimore (4A)	4700	116.0–156.1	169.0–224.7	134.1–180.6	−30.9%	−13.7%
Atlanta (3A)	2830	97.8–125.0	144.5–184.8	113.8–146.8	−32.4%	−14.7%
Houston (2A)	1440	83.4–102.6	125.5–156.5	97.7–122.8	−33.9%	−15.7%
Miami (1A)	140	68.5–84.1	105.8–132.4	81.1–102.7	−35.9%	−17.0%

Place data (RC: 1518 m^3 vs. mass timber: 759 m^3). The general conditions estimate for RC reflects the schedule extension to 26 months and the corresponding additional winter heating season. The relatively wide prediction interval for RC reflects the inherently greater variability of cast-in-place construction practices; future framework refinement could narrow this width by incorporating project-specific field data on formwork turnover and curing schedules.

3.3.4. Framework transferability

The Bakers Place validation demonstrates two important characteristics of the dual-track methodology. The methodology achieves high predictive accuracy across all three structural systems, with the observed Bakers Place values agreeing closely with the predicted ranges for mass timber, structural steel, and reinforced concrete. The well-defined equipment operations and predictable installation sequences — particularly for systems dominated by prefabrication and rapid on-site assembly — align well with the dual-track modeling assumptions.

The successful validation on the Bakers Place across the three structural systems with a consistent climate zone supports the methodology's applicability beyond the original calibration cases. The dual-track framework provides a transferable methodology for A5 energy quantification that can be adapted to project-specific parameters while maintaining methodological consistency. Future framework refinements incorporating measured field data on formwork efficiency and curing schedules could further narrow the RC prediction interval.

3.4. Climate sensitivity analysis

To assess the generalizability of the dual-track framework beyond the U.S. Midwest cold climate (ASHRAE Climate Zone 5A) on which the calibration cases are located, the analysis was extended across five ASHRAE 169-2020 representative cities spanning Climate Zones 1A through 5A. The non-heating components of A5 energy (deep foundation, concrete structures, and superstructure installation) are climate-invariant and remain at the values reported in Table 5. The temporary-heating component scales with city-specific heating degree days (HDD), drawn from NOAA TMY3 30-year normals, and is propagated through the Monte Carlo framework of Section 2.3.2. Table 8 presents the resulting A5 energy intensities.

Two findings emerge. First, the mass timber A5 advantage holds across all five climate zones studied. Second — and contrary to the intuitive expectation that mass timber's benefit derives primarily from cold-climate construction-schedule compression — the advantage *widens* as climate warms: MT versus RC grows from 29.5% in Milwaukee (5A) to 35.9% in Miami (1A), and MT versus Steel from 12.9% to 17.0% over the same range. The mechanism is structural rather than thermal. Reinforced concrete carries a climate-invariant overhead of approximately +52 MJ/m^2 relative to mass timber, driven by the 2.0× foundation volume requirement and cast-in-place superstructure concrete pumping energy. As heating energy approaches zero in hot zones, this fixed structural gap occupies a proportionally larger share of total A5 energy, amplifying rather than diminishing the mass timber advantage. The same mechanism, to a smaller degree, explains the widening MT-versus-Steel gap.

This finding suggests that the carbon-mitigation case for mass timber, often framed primarily through embodied product-stage emissions, is supplemented by an A5-stage advantage that is robust across the continental U.S. climate range and does not depend on the cold-climate context of the original case studies.

4. Conclusions

This study established a dual-track A5 energy assessment framework to address the underquantification of the A5 construction stage in current LCA practice, by quantifying construction-stage energy consumption across mass timber, reinforced concrete, and structural steel building systems. Based on construction data from two large-scale mass timber projects (INTRO: 60,666 m^2; Ascent: 45,838 m^2), the methodology yields an A5 energy intensity of 139–199 MJ/m^2 for mass timber buildings located in ASHRAE Climate Zone 5A (U.S. Midwest, cold-humid), approximately 30% lower than functionally equivalent reinforced concrete and approximately 13% lower than structural steel for cases in the same climate. The companion Climate Sensitivity Analysis (Section 3.4) shows that the mass timber advantage holds across ASHRAE Climate Zones 1A through 5A and in fact widens modestly in warmer climates, although the absolute A5 totals decline substantially as temporary-heating demand diminishes. Independent validation using the Bakers Place building confirmed that the observed values for all three structural systems (mass timber 173.0, structural steel 180.1, and reinforced concrete 220.9 MJ/m^2) lie within their respective 90% credible intervals predicted by the framework.

The results reveal several important findings. In cold-climate projects, temporary heating dominates A5 energy consumption, accounting for 52%–60% of total site energy. This share diminishes substantially in warmer climates (Section 3.4), but where it applies, it suggests that optimizing construction schedules to reduce the number of winter heating seasons may yield greater A5 energy reductions than optimizing any individual construction operation. Vertical transport operations constitute the decisive factor in structural installation energy, while mechanical fastener energy proves negligible (<0.2%). This study also quantifies, for the first time, the learning-curve effects in CLT installation (44% productivity improvement), indicating that mass timber construction holds significant potential for further schedule compression, which would in turn reduce temporary heating demand. At the methodological level, the dual-track estimation approach (theory-based lower bound plus schedule-based upper bound) overcomes the limitations of traditional single-point estimates by providing a defensible energy range, and Monte Carlo simulation (n = 10,000) provides uncertainty quantification with 90% credible intervals.

Although A5 energy is commonly simplified as approximately 3% of total life-cycle energy in current practice, this study demonstrates that A5 energy intensities are substantially higher than this assumption suggests, and that significant optimization potential exists—particularly through construction schedule management in cold-climate regions. Moreover, as the building sector decarbonizes product-stage emissions through lower-carbon materials and manufacturing processes, the relative share of construction-stage energy is expected to grow, making A5 quantification increasingly relevant.

This study evaluates A5 as a standalone module and does not address other ISO 21930 life-cycle stages; claims about A5's relative weight within the whole life cycle therefore lie beyond the present scope. The calibration cases (INTRO, Ascent, Bakers Place) are all located in the U.S. Midwest cold-climate zone (ASHRAE Zone 5A); while Section 3.4 extends the framework across Zones 1A through 5A using HDD-scaled heating energy and shows the mass timber advantage to be robust across this range, the underlying calibration data for non-heating components (deep foundation, concrete, superstructure installation) remain drawn from cold-climate projects, and warm-climate construction practices (e.g., reduced reliance on temporary enclosure, and introduction of construction-stage cooling not modeled here) may modestly affect non-heating coefficients. Foundation systems cover only raft and pile foundations, with additional types remaining unquantified. Monte Carlo parameters are calibrated from limited observations, and variability in contractor practices may affect prediction accuracy. The methodology is based on conventional diesel-powered equipment; as electric construction equipment becomes prevalent, energy conversion coefficients will require updating. Additionally, all energy consumption is reported in primary energy units (MJ) without differentiation by energy source carbon intensity; future research should extend the framework to a CO_2e-based assessment to enable direct comparison with product-stage carbon benchmarks. Future research should also prioritize expanding climate-zone coverage with field-measured (rather than HDD-scaled) heating data from warm-climate projects, incorporating data from contractors of varying scales, and tracking energy data for electric equipment and renewable-energy temporary facilities.

Overall, this study provides a validated framework for A5-stage energy assessment of large-scale mass timber buildings calibrated against cold-climate cases and extended via climate-sensitivity analysis to ASHRAE Zones 1A through 5A, while also demonstrating its potential for application to reinforced concrete and structural steel systems.

CRediT authorship contribution statement

Baowen Zhang: Writing – review & editing, Writing – original draft, Visualization, Validation, Software, Methodology, Formal analysis. **Hongmei Gu:** Writing – review & editing, Conceptualization. **Paul Crovella:** Writing – review & editing, Supervision, Resources, Funding acquisition, Conceptualization.

Declaration of competing interest

The authors declare that they have no known competing financial interests or personal relationships that could have appeared to influence the work reported in this paper.

Acknowledgments

This research is supported by the State University of New York College of Environmental Science and Forestry and USDA Forest Service, Forest Products Laboratory. During the preparation of this work, the authors used Claude (Anthropic) to assist with grammar review and language enhancement. After using this tool/service, the authors reviewed and edited the content as needed and take full responsibility for the content of the publication.

Data availability

Data will be made available on request.

References

[1] Henrik Jepsen, Magnus Lundgren, Kai Monheim, Hayley Walker (Eds.), Appendix: The Paris agreement, in: Negotiating the Paris Agreement: The Insider Stories, Cambridge University Press, 2021, pp. 342–364, http://dx.doi.org/10.1017/9781108886246.018.

[2] N. Kisku, H. Joshi, M. Ansari, S.K. Panda, Sanket Nayak, Sekhar Chandra Dutta, A critical review and assessment for usage of recycled aggregate as sustainable construction material, Constr. Build. Mater. (ISSN: 0950-0618) 131 (2017) 721–740, http://dx.doi.org/10.1016/j.conbuildmat.2016.11.029.

[3] Hui Yan, Qiping Shen, Linda C.H. Fan, Yaowu Wang, Lei Zhang, Greenhouse gas emissions in building construction: A case study of one peking in Hong Kong, Build. Environ. (ISSN: 0360-1323) 45 (4) (2010) 949–955, http://dx.doi.org/10.1016/j.buildenv.2009.09.014.

[4] Carlo Ingrao, Flavio Scrucca, Caterina Tricase, Francesco Asdrubali, A comparative life cycle assessment of external wall-compositions for cleaner construction solutions in buildings, J. Clean. Prod. (ISSN: 0959-6526) 124 (2016) 283–298, http://dx.doi.org/10.1016/j.jclepro.2016.02.112.

[5] Amitha Jayalath, Satheeskumar Navaratnam, Tuan Ngo, Priyan Mendis, Nick Hewson, Lu Aye, Life cycle performance of cross laminated timber mid-rise residential buildings in Australia, Energy Build. (ISSN: 0378-7788) 223 (2020) 110091, http://dx.doi.org/10.1016/j.enbuild.2020.110091.

[6] Hui Zhu, Shuenn-Ren Liou, Pi-Cheng Chen, Xia-Yun He, Meng-Lin Sui, Carbon emissions reduction of a circular architectural practice: A study on a reversible design pavilion using recycled materials, Sustainability (ISSN: 2071-1050) 16 (5) (2024) 1729, http://dx.doi.org/10.3390/su16051729.

[7] Raphaela Ivanica, Michael Risse, Gabriele Weber-Blaschke, Klaus Richter, Development of a life cycle inventory database and life cycle impact assessment of the building demolition stage: A case study in Germany, J. Clean. Prod. (ISSN: 0959-6526) 338 (2022) 130631, http://dx.doi.org/10.1016/j.jclepro.2022.130631.

[8] Donwoo Lee, Jeonghyun Kim, Seungjae Lee, Optimal design of truss structures for sustainable carbon emission reduction in Korean construction, Sustainability (ISSN: 2071-1050) 16 (14) (2024) 5830, http://dx.doi.org/10.3390/su16145830.

[9] Gabriel Felmer, Rodrigo Morales-Vera, Rodrigo Astroza, Ignacio González, Maureen Puettmann, Mark Wishnie, A lifecycle assessment of a low-energy mass-timber building and mainstream concrete alternative in central Chile, Sustainability (ISSN: 2071-1050) 14 (3) (2022) 1249, http://dx.doi.org/10.3390/su14031249.

[10] Hussam Alghamdi, H. Shoukry, Md Uzzal Hossain, Priyadharshini Perumal, Adeolu Adediran, Aref A. Abadel, Ahmed S. Youssef, Reuse of waste rockwool for improving the performance of LC3-based mortars made with natural and recycled aggregates for sustainable building solutions, J. Build. Eng. (ISSN: 2352-7102) 93 (2024) 109881, http://dx.doi.org/10.1016/j.jobe.2024.109881.

[11] Aayusha Chapagain, Paul Crovella, Building sustainable futures: Evaluating embodied carbon emissions and biogenic carbon storage in a cross-laminated timber wall and floor (honeycomb) mass timber building, Sustainability (ISSN: 2071-1050) 17 (12) (2025) 5602, http://dx.doi.org/10.3390/su17125602.

[12] Paul Crovella, William Smith, Jacek Bartczak, Experimental verification of shear analogy approach to predict bending stiffness for softwood and hardwood cross-laminated timber panels, Constr. Build. Mater. (ISSN: 0950-0618) 229 (2019) 116895, http://dx.doi.org/10.1016/j.conbuildmat.2019.116895.

[13] P.D. Kremer, M.A. Symmons, Mass timber construction as an alternative to concrete and steel in the Australia building industry: a PESTEL evaluation of the potential, Int. Wood Prod. J. (ISSN: 2042-6453) 6 (3) (2015) 138–147, http://dx.doi.org/10.1179/2042645315y.0000000010.

[14] Michael Green, Jim Taggart, Wood innovation and design centre: Prince george, Canada, in: Tall Wood Buildings: Design, Construction and Performance, Third and expanded, Birkhäuser, Basel, ISBN: 9783035628340, 2025, pp. 128–137, http://dx.doi.org/10.1515/9783035628340-019, URL https://doi.org/10.1515/9783035628340-019.

[15] Galina Churkina, Alan Organschi, Christopher P.O. Reyer, Andrew Ruff, Kira Vinke, Zhu Liu, Barbara K. Reck, T.E. Graedel, Hans Joachim Schellnhuber, Buildings as a global carbon sink, Nat. Sustain. (ISSN: 2398-9629) 3 (4) (2020) 269–276, http://dx.doi.org/10.1038/s41893-019-0462-4.

[16] Shaobo Liang, Hongmei Gu, Richard Bergman, Environmental life-cycle assessment and life-cycle cost analysis of a high-rise mass timber building: A case study in Pacific northwestern united states, Sustainability (ISSN: 2071-1050) 13 (14) (2021) 7831, http://dx.doi.org/10.3390/su13147831.

[17] WoodWorks Innovation Network, Project gallery, 2026, (Accessed 12 March 2026) https://www.woodworksinnovationnetwork.org/.

[18] Zhuocheng Duan, Qiong Huang, Qi Zhang, Life cycle assessment of mass timber construction: A review, Build. Environ. (ISSN: 0360-1323) 221 (2022) 109320, http://dx.doi.org/10.1016/j.buildenv.2022.109320.

[19] Atsushi Takano, Annette Hafner, Lauri Linkosalmi, Stephan Ott, Mark Hughes, Stefan Winter, Life cycle assessment of wood construction according to the normative standards, Eur. J. Wood Wood Prod. (ISSN: 1436-736X) 73 (3) (2015) 299–312, http://dx.doi.org/10.1007/s00107-015-0890-4.

[20] Ambrose Dodoo, Leif Gustavsson, Roger Sathre, Lifecycle carbon implications of conventional and low-energy multi-storey timber building systems, Energy Build. (ISSN: 0378-7788) 82 (2014) 194–210, http://dx.doi.org/10.1016/j.enbuild.2014.06.034.

[21] A.M. Moncaster, F. Pomponi, K.E. Symons, P.M. Guthrie, Why method matters: Temporal, spatial and physical variations in lca and their impact on choice of structural system, Energy Build. (ISSN: 0378-7788) 173 (2018) 389–398, http://dx.doi.org/10.1016/j.enbuild.2018.05.039.

[22] Francesca Pierobon, Monica Huang, Kathrina Simonen, Indroneil Ganguly, Environmental benefits of using hybrid CLT structure in midrise non-residential construction: An LCA based comparative case study in the U.S. Pacific northwest, J. Build. Eng. (ISSN: 2352-7102) 26 (2019) 100862, http://dx.doi.org/10.1016/j.jobe.2019.100862.

[23] Maureen Puettmann, Francesca Pierobon, Indroneil Ganguly, Hongmei Gu, Cindy Chen, Shaobo Liang, Susan Jones, Ian Maples, Mark Wishnie, Comparative LCAs of conventional and mass timber buildings in regions with potential for mass timber penetration, Sustainability (ISSN: 2071-1050) 13 (24) (2021) 13987, http://dx.doi.org/10.3390/su132413987.

[24] Hangyong Ray Lu, Ali El Hanandeh, Benoit P. Gilbert, A comparative life cycle study of alternative materials for Australian multi-storey apartment building frame constructions: Environmental and economic perspective, J. Clean. Prod. (ISSN: 0959-6526) 166 (2017) 458–473, http://dx.doi.org/10.1016/j.jclepro.2017.08.065.

[25] Ying Liu, Haibo Guo, Cheng Sun, Wen-Shao Chang, Assessing cross laminated timber (CLT) as an alternative material for mid-rise residential buildings in cold regions in China2014a life-cycle assessment approach, Sustainability (ISSN: 2071-1050) 8 (10) (2016) 1047, http://dx.doi.org/10.3390/su8101047.

[26] Katsuyuki Nakano, Masahiko Karube, Nobuaki Hattori, Environmental impacts of building construction using cross-laminated timber panel construction method: A case of the research building in kyushu, Japan, Sustainability (ISSN: 2071-1050) 12 (6) (2020) 2220, http://dx.doi.org/10.3390/su12062220.

[27] Leif Gustavsson, Anna Joelsson, Roger Sathre, Life cycle primary energy use and carbon emission of an eight-storey wood-framed apartment building, Energy Build. (ISSN: 0378-7788) 42 (2) (2010) 230–242, http://dx.doi.org/10.1016/j.enbuild.2009.08.018.

[28] Chia-Lung Yeh, Toshiaki Sato, Applicability of mid-rise timber structures in the metropolitan area, in: World Conference on Timber Engineering 2025, in: WCTE 2025, World Conference On Timber Engineering 2025, 2025, pp. 195–202, http://dx.doi.org/10.52202/080513-0025.

[29] ISO, ISO 14040:2006 Environmental Management – Life Cycle Assessment – Principles and Framework, Technical report, International Organization for Standardization, Geneva, Switzerland, 2006.

[30] ISO, ISO 14044:2006 Environmental Management – Life Cycle Assessment – Requirements and Guidelines, Technical report, International Organization for Standardization, Geneva, Switzerland, 2006.

[31] ISO, ISO 21930:2017 Sustainability in Buildings and Civil Engineering Works – Core Rules for Environmental Product Declarations of Construction Products and Services, Technical report, International Organization for Standardization, Geneva, Switzerland, 2017.

[32] ASHRAE/ICC, Proposed Standard 240P – Quantification of Life Cycle Greenhouse Gas Emissions of Buildings (Public Review Draft), American Society of Heating, Refrigerating and Air-Conditioning Engineers and International Code Council, Atlanta, GA / Washington, DC, 2024, https://osr.ashrae.org (Accessed 12 March 2026).

[33] Yung-ching Chan, Comparison of mass timber structure and RC structure with regard to sustainability by life cycle assessment, Appl. Comput. Eng. (ISSN: 2755-273X) 61 (1) (2024) 255–261, http://dx.doi.org/10.54254/2755-2721/61/20240973.

[34] Osama A.B. Hassan, Nour Emad A.A., Gabriel Abdulahad, A comparative study between glulam and concrete columns in view of design, economy and environment, Case Stud. Constr. Mater. (ISSN: 2214-5095) 16 (2022) e00966, http://dx.doi.org/10.1016/j.cscm.2022.e00966.

[35] Gordian, RSMeans Data: Building Construction Costs with RSMeans Data 2022, 80, Gordian / John Wiley & Sons, ISBN: 9781955341219, 2022.

[36] Uniben Yao Ayikoe Tettey, Ambrose Dodoo, Leif Gustavsson, Effect of different frame materials on the primary energy use of a multi storey residential building in a life cycle perspective, Energy Build. (ISSN: 0378-7788) 185 (2019) 259–271, http://dx.doi.org/10.1016/j.enbuild.2018.12.017.

[37] Phil Lewis, Michael Leming, William Rasdorf, Impact of engine idling on fuel use and CO2 emissions of nonroad diesel construction equipment, J. Manag. Eng. (ISSN: 1943-5479) 28 (1) (2012) 31–38, http://dx.doi.org/10.1061/(asce)me.1943-5479.0000068.

[38] Simaan M. AbouRizk, Daniel W. Halpin, Statistical properties of construction duration data, J. Constr. Eng. Manag. (ISSN: 1943-7862) 118 (3) (1992) 525–544, http://dx.doi.org/10.1061/(asce)0733-9364(1992)118:3(525).

[39] Supriya Goel, Michael I. Rosenberg, ANSI/ASHRAE/IES Standard 90.1-2010 Performance Rating Method Reference Manual, Technical report, Office of Scientific and Technical Information (OSTI), 2016, http://dx.doi.org/10.2172/1253882.

[40] Cong Zhang, Kiho Jung, Richard Harris, Wen-Shao Chang, Drive-in torque for self-tapping screws into timber, Proc. Inst. Civ. Eng. - Constr. Mater. (ISSN: 1747-6518) 175 (1) (2022) 31–43, http://dx.doi.org/10.1680/jcoma.18.00087.

[41] T.P. Wright, Factors affecting the cost of airplanes, J. Aeronaut. Sci. (ISSN: 1936-9956) 3 (4) (1936) 122–128, http://dx.doi.org/10.2514/8.155.

[42] Anthony Mirando, Lameck Onsarigo, Estimating mass timber projects, in: Managing Mass Timber, Routledge, ISBN: 9781003482543, 2025, pp. 73–95, http://dx.doi.org/10.1201/9781003482543-3.

[43] U.S. Environmental Protection Agency, Emission Factors for Greenhouse Gas Inventories, Center for Corporate Climate Leadership, GHG Emission Factors Hub, 2024, URL https://www.epa.gov/climateleadership/ghg-emission-factors-hub.

[44] U.S. Environmental Protection Agency, eGRID year 2023 summary tables, 2024, URL https://www.epa.gov/egrid Emissions & Generation Resource Integrated Database.

[45] Nadia Zahabi, Hongmei Gu, Meng Gong, Janet Blackadar, A comparative whole-building life cycle assessment of the four framing systems of the bakers place building using the tally LCA tool, Buildings (ISSN: 2075-5309) 15 (7) (2025) 1192, http://dx.doi.org/10.3390/buildings15071192.